Talanta 134 (2015) 8–15

Contents lists available at ScienceDirect

Talanta

journal homepage: www.elsevier.com/locate/talanta

Determination of imidacloprid in water samples via photochemically induced fluorescence and second-order multivariate calibration

Edwar Fuentes *, Camila Cid, María E. Báez

Departamento de Química Inorgánica y Analítica, Facultad de Ciencias Químicas y Farmacéuticas, Universidad de Chile, Santiago, Casilla 233, Chile

ARTICLE INFO

Article history:
Received 28 July 2014
Received in revised form
7 November 2014
Accepted 10 November 2014
Available online 15 November 2014

Keywords:
Imidacloprid
Water
Photo-induced fluorescence
Multivariate calibration

ABSTRACT

This paper presents a new method for the determination of imidacloprid in water samples; one of the most widely used neonicotinoid pesticides in the farming industry. The method is based on the measurement of excitation–emission spectra of photo-induced fluorescence (PIF-EEMs) associated with second-order multivariate calibration with a parallel factor analysis (PARAFAC) and unfolded partial least squares coupled to residual bilinearization (U-PLS/RBL). The second order advantage permitted the determination of imidacloprid in the presence of potential interferences, which also shows photo-induced fluorescence (other pesticides and/or unexpected compounds of the real samples). The photoreaction was performed in 100-μl disposable micropipettes. As a preliminary step, solid phase extraction on C18 (SPE-C18) was applied to concentrate the analyte and diminish the limit of detection. The LOD was approximately 1 ng mL^{-1}, which is suitable for detecting imidacloprid in water according to the guidelines established in North America and Europe. The PIF-EEMs coupled to PARAFAC or U-PLS/RBL was successfully applied for the determination of imidacloprid in different real water samples, with an average recovery of 101 ± 10%.

1. Introduction

Neonicotinoid insecticides are a new group of pesticides with properties that allow for their systemic distribution within plants after being absorbed by the leaves or roots. The major modes of application of these compounds are spraying and seed dressing, especially to control pests in crops, such as cereals, soybeans, corn and several fruits and vegetables. Due to their high efficiency, good selectivity against a large number of pests and insects, low mammalian toxicity, and high versatility in a wide range of agricultural practices, they have become dominant pesticides [1]. Globally, 60% of neonicotinoids are used in seed dressing. However, the widespread adoption of these compounds is also due to their flexibility of use, including as foliar sprays on soft fruits; arable crops, such as soya; and in gardens as a flower spray [2].

Imidacloprid [1-(6-chloro-3-pyridylmethyl)-*N*-nitroimidazolidin-2-ylideneamine] belongs to a new group of active ingredients and was first introduced to the market by Bayer in 1991. It is currently the most widely used neonicotinoid in the farming industry. Due to its polarity, the extensive use of imidacloprid may cause pollution of surface or groundwater via runoff or percolation and also via the drainage of treated soil. In surface water, imidacloprid may degrade due to sunlight, pH, and temperature, producing several compounds that may be hazardous to the health of vertebrates, mammals and humans [3]. However, its transport into groundwater makes this compound more persistent and may affect several aquatic organisms [4]. Moreover, neonicotinoid pesticides could have an adverse effect on the population of bees, causing the so-called "colony collapse disorder", which is characterized by sudden depopulation of hives by worker bees and the subsequent death of the larvae and queen. Along with the decline in honey production, the loss of pollinators has had a negative impact on the reproduction of multiple crops [5,6]. Thus, the use of these pesticides in agriculture also has indubitable repercussions on the environment and the quality of natural waters, which has become a serious environmental concern.

Monitoring the environmental impact of neonicotinoid insecticides in matrix environments, such as natural water, requires sensitive analytical methods. The low concentration levels of imidacloprid that may be present in these types of samples make sample treatments that involve extraction and concentration steps necessary. The extraction of imidacloprid from aqueous samples has primarily been performed using liquid–liquid extraction (LLE) [7] and solid phase extraction (SPE) on C18 [7–10]. On the other hand, due to its low volatility and relatively high hydrophilicity, the determination of imidacloprid in environmental water samples

* Corresponding author. Tel.: +56 229782830.
E-mail address: edfuentes@ciq.uchile.cl (E. Fuentes).

http://dx.doi.org/10.1016/j.talanta.2014.11.017
0039-9140/

has primarily been performed using liquid chromatography methods with UV or diode array detection [11–15], mass spectrometry detection [16–18], ion chromatography [19] and micellar electrokinetic chromatography [8].

The summarized conventional analytical approaches applied for imidacloprid determination in water samples require a large amount of solvent and produce a large amount of waste due to sample preparation and chromatographic analysis. Alternative methods based on the fluorimetry of a photoproduct of imidacloprid produced after the UV irradiation of an aqueous imidacloprid solution have been proposed for water analysis. In aqueous media, imidacloprid does not exhibit native fluorescence; however, its irradiation with UV light results in a fluorescent signal. The fluorescent photoproduct generated in a basic aqueous media has been previously isolated and identified as 1-(6-chloro-3-pyridylmethyl)-2-(hydroxyimino)-3,4-didehydroimidalozolidene, which exhibits native fluorescence [20]. In this work, the authors proposed a fluorimetric method for the determination of imidacloprid in water after its irradiation. Subsequently, Vílchez et al. [21] presented a flow injection alternative to the method using a homemade continuous photochemical reactor to irradiate the sample while it was circulated through a PTFE tube. In another study, López Flores et al. [22] proposed a method for determining imidacloprid in peppers and environmental water samples that combines photochemically induced fluorescence, performed in-line, with solid phase spectroscopy of the fluorescent compound retained on a C18 filled flow-cell. The reported limits of detection were 4.1 and 1.8 $\mu g\, l^{-1}$ for injection volumes of 100 and 640 μl, respectively. A similar method for the in-line determination of imidacloprid in water samples was developed more recently by Araujo et al. [23], who reported a limit of detection of 5.3 $\mu g\, l^{-1}$ with an injection volume of 100 μl. In a different approach, Subhani et al. [19] proposed the determination of imidacloprid and carbendazim in water samples using a post-column photochemical reactor with alkaline medium and fluorescence detection after the ion chromatography separation of analytes. The limit of detection reported for imidacloprid by the authors was 7.8 $\mu g\, l^{-1}$.

However, the relevance of these methods has been limited by their lack of selectivity, especially when chemically similar compounds must be analyzed in a complex matrix. One approach to improve the analytical selectivity in this matrix would be the use of excitation–emission fluorescence measurements (three-way data set), in conjunction with different chemometric algorithms as a parallel factor analysis (PARAFAC) and unfolded partial least square with residual bilinearization (U-PLS/RBL) to build a second-order calibration method. These methods permit the resolution of analytical signals without the use of chromatography and the resolution of spectra of target compounds from a complex background signal and overlapping spectral interferences that are not included in the calibration set (known as the second-order advantage) [24]. This characteristic helps minimize sample pretreatment, which is primarily used to concentrate the analyte and reduce the limit of detection. Moreover, the use of excitation–emission fluorescence data also improves this analytical characteristic and avoids increasing the volume of sample to be analyzed.

Despite the capability of chemometric methods, there are no available reports on the determination of imidacloprid in water samples through photochemically induced fluorescence spectroscopy coupled to multivariate calibration. In this work, PARAFAC and U-PLS/RBL methods were applied to determine imidacloprid in different water samples using photochemically induced fluorescence excitation–emission matrices (PIF-EEMs) in presence of other pesticides (clothianidin, thiamethoxam, fipronil, carbofuran, carbaryl, fenvalerate and atrazine) and/or dissolved fluorophores presents in water samples as potential interferences. The UV irradiation of samples was performed using disposable micropipettes. Solid phase extraction (SPE) on C18 was used as sample preparation step. The predicted PARAFAC and U-PLS/RBL concentrations were compared with those obtained using high-performance liquid chromatography (HPLC) with UV–vis detection. The method was applied for the analysis of different water samples (mineral, drinking, well and irrigation ditch).

2. Theory: figures of merit in multivariate calibration.

In multivariate calibration, figures of merit are related to the concept of multivariate net analyte signal (NAS) [25,26]. This concept involves the decomposition of the total spectrum of a given sample (x) into two orthogonal parts: one part that can be uniquely assigned to the analyte of interest (the net analyte signal, designated x^*) and the remaining part that contains the contributions from the other components, which may be different than expected or unexpected sample components (x_{other}), as indicated in Eq. (1):

$$x = x_n^* + x_{other} = c_n \cdot s_n^* + x_{other} \quad (1)$$

where x_n^* and s_n^* are the net analyte signals (vector signal) corresponding to a given sample and to a sample having the nth analyte at unit concentration, respectively, and c_n is the analyte concentration. If matrix-like net analyte signals are implied, Eq. (2) is applied

$$X_n^* = c_n \cdot S_n^* \quad (2)$$

The expressions for the sensitivity (S_n) are obtained from the norm of the net analyte signal at unit concentration $s_n = \|s_n^*\|$ or $S_n = \|S_n^*\|$. Conversely, for an inverse model the sensitivity is defined as $S_n = \|s_n^*\|^{-1}$ or $S_n = \|S_n^*\|^{-1}$.

When the second-order advantage is used, the sensitivity is sample-specific and cannot be defined for the multivariate method as a whole. In this case, an average value for the set of samples can be estimated and reported [25]. The analytical sensitivity, γ_n, appears to be more useful than S_n and is defined, analogous to univariate calibration, as the quotient between S_n and the instrumental noise level (s_x). Its inverse, γ_n^{-1}, establishes the minimum concentration difference that can be appreciated across the linear range and is independent of the instrument or scale [26]. Thus, the limit of detection (LOD_n) can be gathered from the expression $LOD_n = 3\ \gamma_n^{-1}$. In addition to S_n as an average value over a test sample set, LOD_n is also reported as an average figure of merit.

3. Experimental

3.1. Reagents and solutions

Imidacloprid, clothianidin, thiamethoxam and fipronil were of high purity grade and obtained from Sigma-Aldrich (St. Louis. MO, USA). NaCl, NaOH and Na_2HPO_4 were of analytical purity grade and obtained from Merck (Darmstadt, Germany). Acetonitrile, methanol and chloroform were of HPLC grade and purchased from Merck (Darmstadt, Germany).

Stock solutions of pure analytes (1000 $\mu g\, mL^{-1}$) and diluted solutions (100 $\mu g\, mL^{-1}$) were prepared in acetonitrile. The stock solutions were stored in amber vials at 4 °C in the dark. Under these conditions, the stock solutions were stable for almost two months.

3.2. Apparatus and software

A Varian Cary-Eclipse luminescence spectrometer (Mulgrave, Australia) equipped with a xenon flash lamp was used to obtain excitation–emission fluorescent measurements. A Hellma

(105.250 QS) quartz cell with a 100-μl inner volume and a 10 × 2-mm light path was used. The classic fluorescence spectra were recorded at λ_{exc} of 355 nm in the λ_{em} range of 365–700 nm every 2 nm at a scanning rate of 600 nm min^{-1}. The EEMs were recorded in the λ_{exc} ranges of 220–400 nm every 5 nm and λ_{em} of 324–550 nm every 2 nm. The widths of the excitation and emission slits were 10 nm. The spectra were saved in ASCII format and transferred to a computer for subsequent manipulation. The routine for data pre-treatment used to eliminate Rayleigh and Raman scattering peaks from the EEMs [27], and subsequent data processing was implemented in MATLAB [28]. The routines used for the PARAFAC and U-PLS/RBL are available on the internet [29]. All the algorithms were implemented using the graphical interface of the MVC2 toolbox [30], which is also available on the internet [31].

High-performance liquid chromatography with a diode array detector (HPLC-DAD) analysis was performed on a liquid chromatograph equipped with a Waters 600 HPLC pump, a Waters 996 diode array detector and a Waters 717 auto sampler (Milford, MA, USA). The column was an Eclipse XDB C18 (150 × 4.6-mm ID, 5-mm particle size) from Agilent (Santa Clara, USA) the temperature was maintained at 35 °C during the analysis. The mobile phase was a mixture of acetonitrile (A) and water acidified with phosphoric acid at pH 2.6 (B) at a flow rate of 1.2 mL min^{-1}. The following gradient program was used: 0–1 min linear gradient from 30% to 75% A; 10–14 min 75% A isocratic; and back to the initial condition: 15–16 min linear gradient 75–30% A; 16–22 min 30% A isocratic. This program was used for the separation of imidacloprid, clothianidin, thiamethoxam and fipronil. An injection volume of 20 μl was employed. Detection at 270 nm was used for the quantification of imidacloprid.

3.3. Sample treatment and extraction of imidacloprid

Water samples were collected in dark glass bottles previously cleaned with hydrochloric acid and washed with deionized water. The samples were stored in the dark at 4 °C until the analysis was performed. Before the SPE procedure, the samples were filtered through a cellulose acetate filter (0.20-μm pore size, Minisart, Sartorious). Potential losses of imidacloprid by adsorption on the filters used were evaluated. No differences were observed in samples spiked before or after this procedure.

For the SPE procedure, C18 cartridges (ENVI-18, 500 mg from Sigma-Aldrich) were conditioned with 3.0 mL of methanol and 3.0 mL of Milli-Q water. Next, 10 mL of a water sample containing imidacloprid was loaded into the conditioned cartridges at a flow rate of 1.2 mL min^{-1} without allowing the column bed to become dry, and the eluent was discarded. The cartridges were rinsed with 10 mL of Milli-Q water, dried with nitrogen for 5.0 min and then eluted with 3.0 mL of methanol. The methanol eluent was evaporated to dryness using a mild nitrogen stream over a dry bath at 40 °C. The residue was dissolved in 200 μl of 0.01 M phosphate buffer, pH 11.5, for irradiation with UV light or in 200 μl of acetonitrile for a HPLC analysis.

3.4. Procedure for the determination of imidacloprid

The UV irradiation was performed using a Vilbert Lourmat lamp (France, model VL-115.G) that operates a tube of 15 W with 254 nm as the spectral line (model T-15.C). A box with an internal coating of aluminum that permitted the maximum reflectance of UV light was placed over the lamp. Due to the short irradiation time applied to the samples, no cooling device was needed, and all experiments were performed at room temperature. A 100-μl aliquot obtained after the extraction procedures described above or a phosphate buffer containing imidacloprid (calibration samples) was aspirated into a 100-μl disposable glass micropipette with a ring mark (Brand, Wertheim, Germany). Then, one end of the micropipette was sealed with hematocrit sealing wax (Brand, Wertheim, Germany) and the other with Parafilm®. The micropipette was placed 1 cm from the UV tube of the lamp and irradiated for 25 s. Subsequently, the Parafilm was removed and the micropipette was cut on the side of the wax using a silica capillary column cutter. The sample was transferred to a quartz cell with a 100-μl inner volume (Hellma, Müllheim, Baden, Germany) to obtain the EEMs.

3.5. Calibration and validation set samples

A calibration set of 6 samples in duplicate was prepared from the diluted solutions at concentrations of 0.1; 0.2; 0.3; 0.4; 0.5 and 0.75 μg mL^{-1} of imidacloprid in phosphate buffer. With the aim of evaluating the predictive capacity of the calibration model in the presence of unexpected constituents, a validation set of 10 samples was prepared in phosphate buffer at concentrations different from those used for calibration and in the presence of clothianidin, thiamethoxam (neonicotinoid pesticides) and fipronil as potential interferences. Table 1 shows the composition of the validation set. All of the samples were irradiated, their EEMs were read and the data were subjected to a second-order data analysis.

3.6. Test sample set

To test the recovery and predictive capacity of the proposed method, a validation set was prepared at 1/50 of the concentration displayed in Table 1. Subsequently, these samples were processed using the SPE procedure described above, irradiated and their EEMs were read and subjected to the second-order data analysis. This test set was also analyzed using HPLC-DAD as a reference method.

4. Results and discussion

4.1. Photochemical induction of fluorescence and EMMs of imidacloprid

The photoreaction was performed in a very simple way using 100-μl disposable glass micropipettes to contain the sample. Although glass can restrict the penetration of ultraviolet rays of wavelengths below 290 nm, the penetration depends on the thickness of glass. Because the wall of the micropipettes is 0.25 mm, ultraviolet radiation can penetrate this wall and reach the contained solution to produce the photoreaction. The use of these disposable micropipettes allows us to work with the small

Table 1
Concentrations in μg mL^{-1} of imidacloprid, clothianidin, thiamethoxam and fipronil in the validation set samples.

Sample	Concentration μg mL^{-1}			
	Imidacloprid	Clothianidin	Thiamethoxam	Fipronil
V1	0.72	0.28	0.38	0.49
V2	0.22	0.05	0.77	1.48
V3	0.44	0.10	0.80	1.49
V4	0.38	0.82	0.19	0.45
V5	0.64	0.69	0.49	0.28
V6	0.50	0.32	0.45	0.57
V7	0.29	0.95	0.65	0.34
V8	0.68	0.03	0.71	1.38
V9	0.20	0.44	0.75	1.07
V10	0.58	0.25	0.27	0.72

sample volumes obtained after concentration, reducing the irradiation time and decreasing the probability of contamination.

According to previously reported studies [22], a 0.01 M Na_2HPO_4/NaOH buffer solution (pH 11.5) was selected as the medium for the photochemical induction of imidacloprid fluorescence. Lower fluorescence intensities were observed using 0.01 M NaOH as an alternative medium. Additionally, the irradiation time was evaluated as a critical variable in this methodology. A solution of imidacloprid at 0.5 μg mL^{-1} in phosphate buffer was irradiated in the range of 5–50 s. The curve of fluorescence with respect to time exhibited an increase of fluorescence, corresponding to the formation of the fluorescent product, and then, a decrease in the signal due to the photodegradation of this product. The maximum signal was obtained at 30 s. However, the calibration curves obtained with irradiation times higher than 25 s exhibited a narrower linearity range. A similar study was conducted with a real water sample (irrigation ditch) that presented potential interferents associated with dissolved organic matter (see Section 4.5). The fluorescence versus time curve was similar in shape and intensity to the above curve, showing that the kinetics and extent of the photoproduct formation were not altered. Thus, 25 s was selected as the irradiation time. Furthermore, the stability of the photoproduct over time after the irradiation and a possible photo bleaching was evaluated by recording the fluorescence from 0 to 60 min every 5 min after the irradiation. The fluorescence intensities did not have significant variations in this period, which demonstrated its stability of the photoproduct over time and the absence of degradation during the measurement of EEM. It is probable that the reduced window of the quartz cell of 100 μl avoid a possible degradation. Anyway, all the EEMs were obtained immediately after the irradiation of the samples.

Fig. 1a–d shows the PIF-EEMs corresponding to samples containing imidacloprid, clothianidin, thiamethoxam and fipronil at 1.0 μg mL^{-1}, which were recorded over a wide spectral range. The broad featureless emission bands from Rayleigh and Raman scattering were eliminated from the EEMs using routines for data pre-treatment [27]. As observed in Fig. 1a, the imidacloprid photoproduct exhibits fluorescence with a maximum intensity at λ_{em} 410 nm and λ_{exc} 345 nm. Among the other compounds considered potential interferences, only clothianidin has a photoproduct with a significant fluorescence, although lower than that of imidacloprid. Moreover, the EEMs of both compounds show a meaningful overlapping in the wavelength range considered (λ_{exc} 220–400 nm; λ_{em} of 324–550 nm). Thus, the determination of imidacloprid in the presence of clothianidin, or other fluorescent interferences present in water samples, requires the use of the second-order advantage achieved using the PARAFC and U-PLS/RBL algorithms.

4.2. Calibration and validation set analysis

The PIF-EEMs of the imidacloprid photoproduct under optimal conditions were recorded for calibration and validation samples. Fig. 2a and b shows contour plots for the calibration sample, where only the studied analyte is present, and the validation sample 9 with interferences, respectively. The anomalous signal observed at excitation wavelengths lower than 250 nm may be related to some impurities of the reagents used and/or light scattering. However, due to its position in the spectral range, these signals do not cause interference in the analysis. Analyses using the PARAFAC and U-PLS/RBL algorithms were applied to these EEMs data. PARAFAC was applied to the three-way data arrays constructed by combining the data matrices for each validation sample with those of the set of calibration samples. The PARAFAC model fits under the non-negativity constraint for loading of the excitation and emission mode. Due to the characteristics of the EEMs data, the initialization was performed via a direct trilinear decomposition (DTLD) of the three-way array. This model obtained allowed us to obtain physically interpretable profiles. The selection of the optimum number of factors was performed using the percentage of fit and core consistency test [32,33]. The number of responsive components was three for each validation samples with a core consistency of 90–100%. Fig. 3 shows the profiles retrieved using PARAFAC in the excitation (Fig. 3a) and emission (Fig. 3b) modes for validation sample 9 in the studied spectral region (λ_{exc} 220–400 nm; λ_{em} of 324–550 nm). The identification of imidacloprid and clothianidin was performed with the aid of these estimated profiles by comparing them with those for an irradiated standard solution. On the other hand, as was discussed previously, the third extracted component may correspond to some impurities of the reagents used and/or light scattering in the spectral region.

In U-PLS/RBL, the selection was performed using the cross-validation method described by Haaland and Thomas [34] over only the calibration set. The optimum number of factors was estimated by calculating the ratio $F(A)=PRESS(A<A^*)/PRESS(A^*)$, where *PRESS* is the predicted error sum of squares, defined as $PRESS=\Sigma_1^I(y_{nominal}-y_{predicted})^2$; A is a trial number of factors; and A^* corresponds to the minimum *PRESS*. The number of optimum factors was selected as the number leading to a probability of less than 75% and $F>1$. In this case, the resulting number of components was three. Unlike PARAFAC, these latent variables do not have any physical interpretation. Furthermore, in addition to the latent components estimated from the calibration set, the analysis of samples from the validation set required the RBL procedure, with the additional components corresponding to the unexpected components present in these samples. Thus, the number of optimum RBL factors for each validation sample, estimated according to the procedure described by Bortolato et al. [35], was two for all of these samples. In this case, U-PLS/RBL considers the profiles of the interferences as additional two components that can be distinguished from those of the analyte. PARAFAC and U-PLS/RBL yielded good predictions of imidacloprid in the validation set with a relative error (REP) of 10%.

4.3. Test set analysis

4.3.1. Recovery of the SPE method

A pre-concentration step based on SPE-C18 was performed to obtain a sensitive method for the quantification of imidacloprid. The test set was subjected to the extraction procedure and subsequently analyzed using HPLC-DAD. As observed in Table 2, application of SPE-C18 led to a mean recovery of imidacloprid of 103%.

4.3.2. Predictive capacity of PARAFAC and U-PLS/RBL and figures of merit

The test set was subjected to the SPE procedure and the photochemically induced fluorescence EEM data generated were analyzed using PARAFAC and U-PLS/RBL. Fig. 2c displays a contour plot of the PIF-EEM for test sample 9 with interferences obtained after SPE-C18. The same irregular signal observed in the calibration and validation samples were present in the test samples at excitation wavelength shorter than 250 nm, without producing interference in the analysis. PARAFAC was applied to the three-way data arrays constructed by combining the data matrices for each test sample with those of calibration samples. The core consistency analysis was applied to select the number of spectral components. The core consistency dropped to a low value when using four spectral components to model the data; thus, as for the validation set, three components were selected as adequate (the core consistency ranged from 82% to 100%). Moreover, the

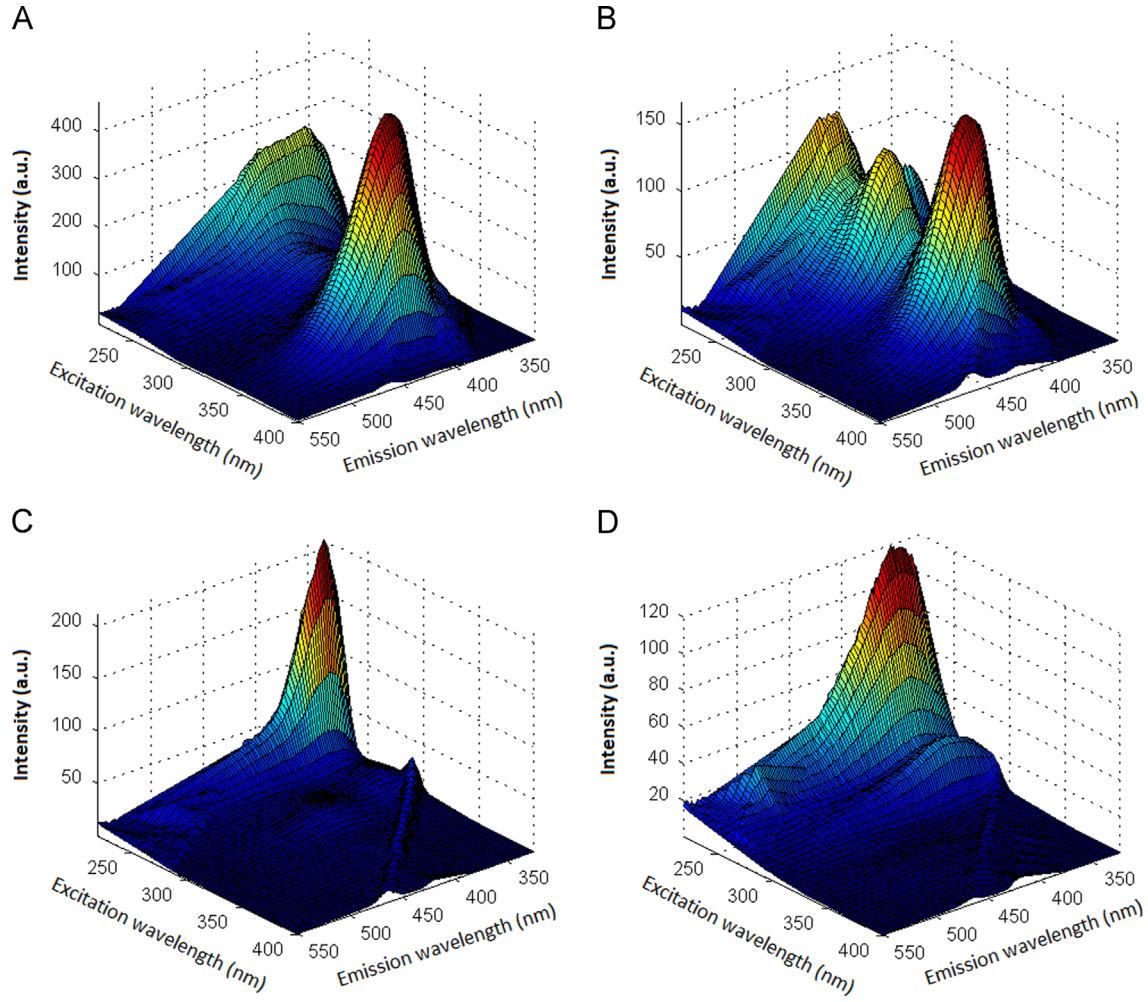

Fig. 1. Three dimensional plots of the excitation–emission matrices obtained after 25 s of irradiation at 254 nm of (A) imidacloprid, (B) clothianidin, (C) thiamethoxam, and (D) fipronil at a concentration of 1 μg mL^{-1} in a pH 11.5, 0.01 M phosphate buffer.

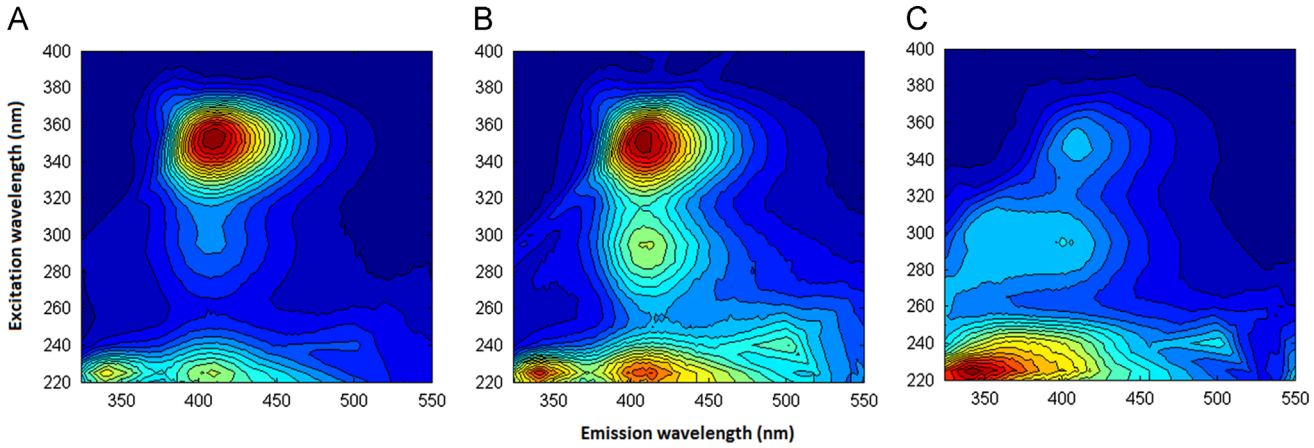

Fig. 2. Contour plots of PIF-EEM for (A) a calibration sample where only imidacloprid is present at 0.5 μg mL^{-1}, (B) validation sample 9 with interferences, and (C) test sample 9 with interferences obtained after SPE-C18.

PARAFAC profiles retrieved in the emission and excitation mode for these samples were practically the same as for the validation samples. The test samples were also evaluated using the U-PLS algorithm. To achieve the second-order advantage, RBL components were required for these samples because they include unexpected components. The number of optimum RBL components was two in all cases. As for the validation set, it can be assumed that U-PLS/RBL considers the profiles of the interferences as additional two components.

The prediction results corresponding to the application of PARAFAC and U-PLS/RBL to the test set subjected to the extraction procedure are listed in Table 2. Additionally, Fig. 4 displays a comparison of these values with those obtained using HPLC as a reference method. No significant differences between the

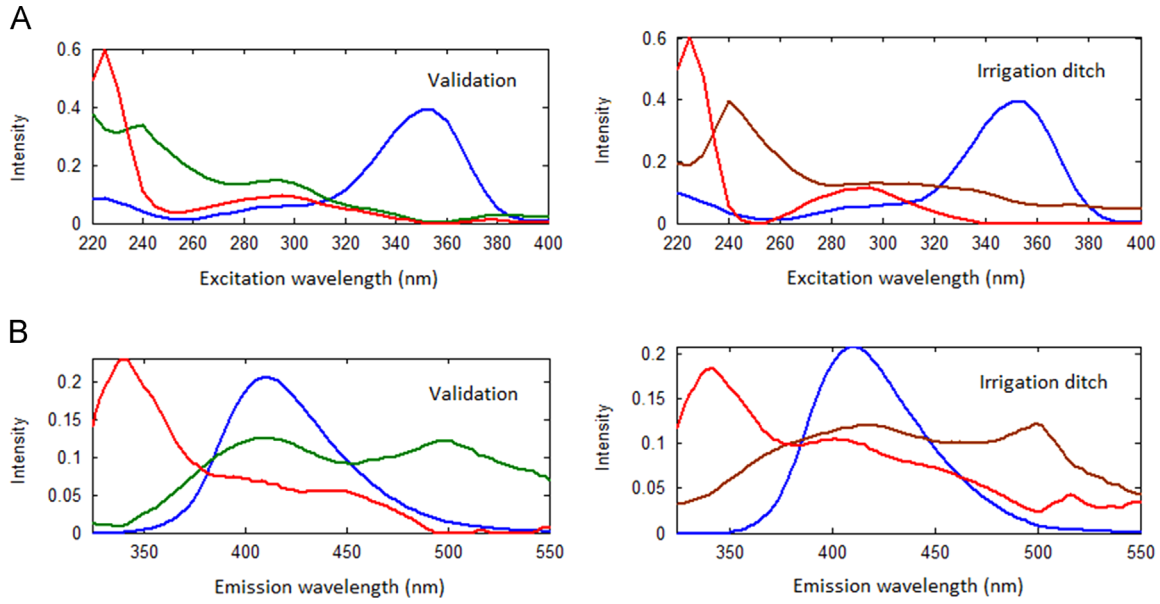

Fig. 3. The PARAFAC recovered profiles for excitation (A) and emission (B) when processing a validation sample (sample 9) and the irrigation ditch water sample together with the calibration set. Component 1 (blue line) matches the imidacloprid spectrum and component 2 (green line) matches clothianidin. For the irrigation ditch water, component 2 (brown line) can be attributed to some common fluorophore present in natural water. In both cases, component 3 (red line) may be related to some impurities in the reagents and/or light scattering. (For interpretation of the references to color in this figure legend, the reader is referred to the web version of this article.)

Table 2
Predictions of imidacloprid in the test set using PARAFAC and U-PLS/RBL and values determined by HPLC-DAD as a reference method. Figures of merit obtained for the three methods.

Sample	Added (ng mL^{-1})	HPLC-DAD	PARAFAC	U-PLS/RBL
V1	14.4	16.5 (115)[a]	15.4 (107)	15.0 (104)
V2	4.4	4.0 (92)	4.2 (95)	4.0 (91)
V3	8.8	8.2 (93)	10.6 (120)	8.8 (100)
V4	7.6	8.3 (109)	7.0 (92)	7.0 (92)
V5	12.8	13.0 (102)	15.2 (119)	13.0 (102)
V6	10.0	10.1 (101)	8.0 (80)	8.2 (82)
V7	5.8	6.3 (109)	6.4 (110)	6.8 (117)
V8	13.6	11.2 (82)	10.8 (79)	9.0 (66)
V9	4.0	4.5 (112)	4.0 (100)	4.6 (115)
V10	11.6	12.9 (111)	9.8 (84)	9.8 (84)
Mean recovery (%)	–	103	99	95
RMSEP (ng mL^{-1})[b]	–	–	1.7	1.5
REP (%) [c]	–	–	18	16
γ^{-1} (μg mL^{-1})	–	0.023	0.010	0.020
LOD=3.3γ^{-1}(ng mL^{-1}) [d]	–	1.5	0.64	1.3

[a] ( ) Values expressed in recoveries %.
[b] Comparison with the values obtained by HPLC-DAD.
[c] Relative error of prediction, REP=100 × RMSEP/c_{mean} where c_{mean} is the mean calibration concentration.
[d] LOD calculated considering the 50-fold pre-concentration factor.

concentrations predicted by both the algorithms and the concentrations obtained from HPLC were observed. Consequently, the theoretical (1,0) points were included within the elliptical joint regions. Nevertheless, SPE-C18 in conjunction with U-PLS/RBL showed the ellipse with the smallest size. The root means square errors of prediction (RMSEP), which is a method for expressing the average error made in predicting the analyte concentration with respect to the reference value delivered using HPLC, was lower than or equal to 18%. Due to the lower dispersion of the results and the values that were more consistent with those determined using HPLC-DAD, SPE-C18 in conjunction with U-PLS/RBL can be deemed the most appropriate method for determining imidacloprid in water samples. On the other hand, the limits of detection of the proposed method were nearly 1 ng mL^{-1} (considering the 50-fold pre-concentration factor: 10 mL initial volume of sample and 0.2 mL final volume), which are adequate to detect the presence of imidacloprid in water samples, according to the water quality guidelines residue limits for imidacloprid established for some countries, notably the USA, Canada, the Netherlands and Sweden (0.13–1.05 ng mL^{-1}) [11]. Note that this value could be even lower if a larger volume of sample is treated. Moreover, the LOD obtained is comparable to that reported using HPLC methods [11,12,15,18] and lower than those reported using PIF and univariate calibration [19,22,23]. A real sample (irrigation ditch water) was fortified at 2 ng mL^{-1} and analyzed in replicates to determine the standard deviation of the predicted concentration and, thus, the LODs, obtaining similar values that those reported in Table 2 ($3.3 \times s_c$= 1.2 ng mL^{-1}, where s_c is the standard deviation of the concentration predicted).

4.4. Effect of additional foreign pesticides

To evaluate the effect of additional foreign compounds on the selectivity of the method, a real sample (irrigation ditch sample) was spiked with a naturally fluorescent pesticide (carbofuran), two pesticides that present photochemically induced fluorescent products (carbaryl and fenvalerate) [36], the easily lixiviable herbicide atrazine and imidacloprid at 0.01 μg mL^{-1} (Table 3). These samples were submitted to SPE-C18-PIF-EEMs and analyzed using PARAFAC and U-PLS/RBL. Fig. 5c displays a contour plot of the PIF-EEM for the spiked sample number 3. A significant overlap between the fluorescence signals of the photoproducts of imidacloprid and carbaryl was observed, which was described by Nahoriak et al. [36]. Nevertheless, the prediction of imidacloprid concentration for this group of samples was satisfactory. The results are summarized in Table 3. As observed, the recoveries were equal or higher than 72% with PARAFAC (two components, core consistency 90–100%) or U-PLS (two or three RBL components). On the other hand, a limit of detection of nearly 1 ng mL^{-1} was also obtained for these samples.

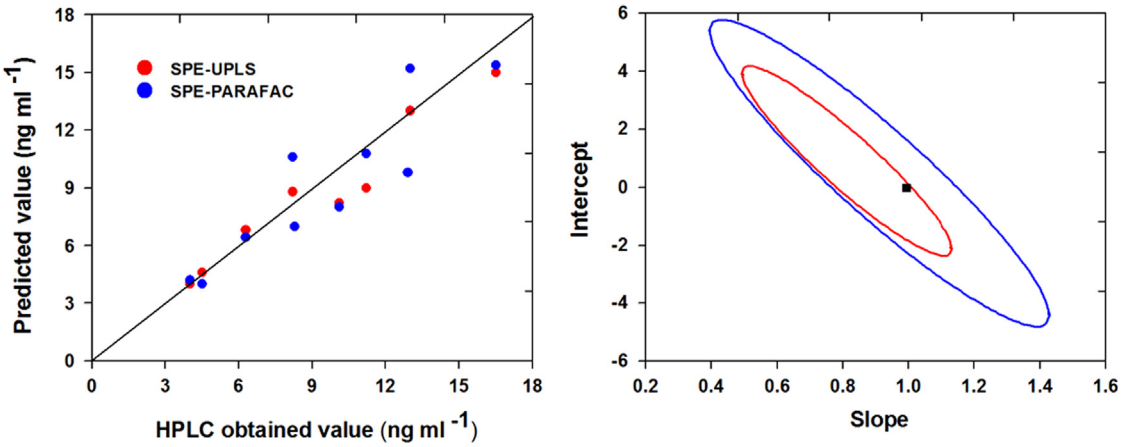

Fig. 4. Plots for imidacloprid predicted concentration with U-PLS/RBL (red circle) and PARAFAC (blue circle) in the test samples as a function of those obtained using HPLC and the corresponding elliptical joint region (at the 95% confidence level). (For interpretation of the references to color in this figure legend, the reader is referred to the web version of this article.)

Table 3
Predictions of imidacloprid and mean LODs in irrigation ditch sample spiked with additional foreign pesticides determined by SPE-C18-PIF-EEMs with PARAFAC and U-PLS/RBL.

Sample	Foreign pesticide added (ng mL^{-1})				Predicted values of imidacloprid [a]	
	Carbofuran	Carbaryl	Fenvalerate	Atrazine	PARAFAC	U-PLS/RBL
1	10	10	50	50	8.0	7.8
2	50	10	10	50	10.6	11.0
3	10	50	50	10	8.8	10.0
4	50	50	10	10	7.2	7.2
LOD (ng mL^{-1}) [b]	–	–	–	–	0.72	1.0

[a] Imidacloprid spiked at 0.01 μg mL $^{-1}$.
[b] LOD calculated considering the 50-fold pre-concentration factor.

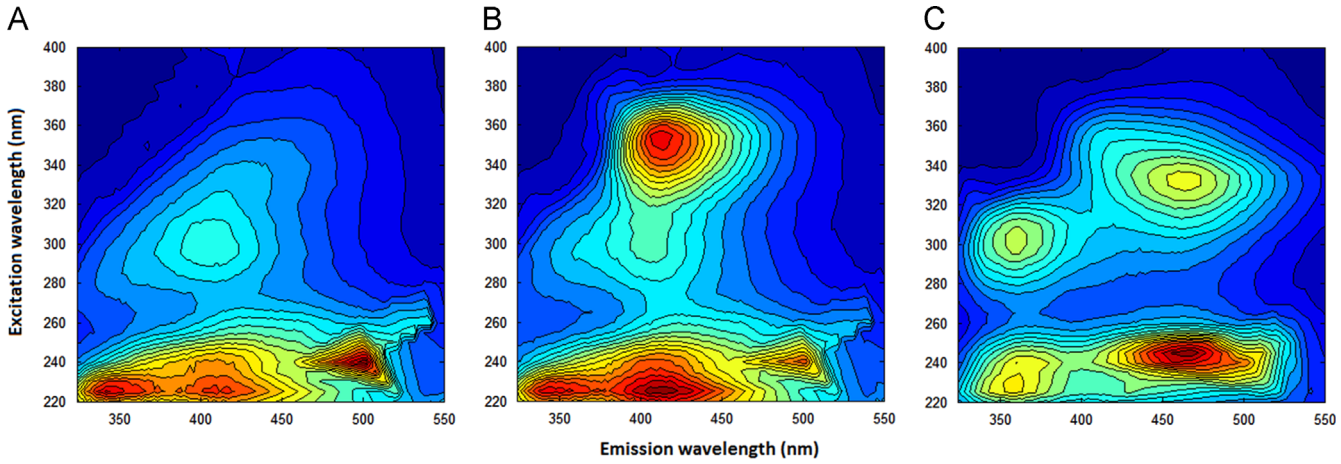

Fig. 5. Contour plot of the PIF-EEM for (A) the irrigation ditch sample, (B) this sample spiked at 0.01 μg mL^{-1} imidacloprid and (C) with additional foreign pesticides (sample 3 in Table 3) obtained after the SPE procedure.

4.5. Analysis of real samples

To evaluate this method in real samples and demonstrate its ability to overcome the interference from the background, five water samples from different origins were analyzed. First, SPE-C18 was applied to these samples, and subsequently, both PARAFAC and U-PLS/RBL were applied to process the PIF-EEMs three-way data and predict the imidacloprid concentrations. As an example, Fig. 5a and b displays a contour plot of the PIF-EEM for the irrigation ditch water sample and the same sample spiked at 0.01 μg mL^{-1} after the SPE procedure, respectively. As observed, the sample shows a considerable fluorescence signal in the same region where the photoproduct of imidacloprid emits. Despite this overlap, the second-order approaches can overcome this drawback. Fig. 3 shows the profiles retrieved for this sample using PARAFAC (core consistency of 93%) in excitation (Fig. 3a) and emission (Fig. 3b) modes. Imidacloprid and two additional components were retrieved. One of them can be attributed to some

Table 4
Recoveries (%) ± standard deviation ($n=3$) of imidacloprid in water samples spiked at 0.01 μg mL $^{-1}$ determined by SPE-C18-PIF-EEMs with PARAFAC and U-PLS/RBL.

Water sample	PARAFAC	U-PLS/RBL
Tap	112 ± 6	106 ± 10
Mineral	102 ± 5	110 ± 10
Well	106 ± 6	102 ± 10
Irrigation ditch	92 ± 5	80 ± 7
Irrigation canal	106 ± 10	96 ± 8

common fluorophores present in natural water [37]. As mentioned above, the third component may be related to some impurities in the reagents used and/or light scattering.

Because the analyte was not detected in these samples, the reliability of these procedures was determined based on a recovery study of the five samples spiked at 0.01 μg mL^{-1}. The results are summarized in Table 4. The recoveries of imidacloprid from spiked water samples were nearly 100% using SPE with PARAFAC (two or three components, core consistency 82–100%) or U-PLS (two RBL components).

5. Conclusions

The feasibility of the fluorimetric determination of imidacloprid in water samples using PIF-EEMs and second-order multivariate calibration was demonstrated. PARAFAC and U-PLS/RBL were applied to the three-way data to achieve the second-order advantage, allowing for the determination of imidacloprid in the presence of interferences in spiked water samples (other fluorescent pesticides and/or dissolved fluorophores present in the water samples). SPE-C18 was applied as a sample preparation step to concentrate the analyte and lower the limit of detection. The values obtained after applying this extraction method and analysis using PARAFAC or U-PLS/RBL do not differ significantly from those obtained using the HPLC analysis. Thus, SPE-C18-PIF-EEMs, in conjunction with PARAFAC or U-PLS/RBL, have been shown to be adequate for routine analysis in the control of the presence of imidacloprid in water samples at the ng mL^{-1} level. Moreover, a sampling rate of five samples per hour makes the method advantageous and represents a suitable alternative to chromatographic methods.

Acknowledgments

The authors gratefully acknowledge the financial support of Fondecyt (Project 1140328).

References

[1] D. Goulson, J. Appl. Ecol. 50 (2013) 977–987.
[2] P. Jeschke, R. Nauen, M. Schindler, A. Elbert, J. Agric. Food Chem. 59 (2011) 2897–2908.
[3] T. Ding, D. Jacobs, B. Lavine, Microchem. J. 99 (2011) 535–541.
[4] D. Hayasaka, T. Korenaga, K. Suzuki, F. Saito, F. Sánchez-Bayo, K. Goka, Ecotoxicol. Environ. Safe 80 (2012) 355–362.
[5] T. Blacquière, G. Smagghe, C.A.M Van Gestel, V. Mommaerts, Ecotoxicology 21 (2012) 973–992.
[6] T. Farooqui, Neurochem. Int. 63 (2013) 122–136.
[7] S. Baskaran, R. Kookana, R. Naidu, J. Chomatogr. A 787 (1997) 271–275.
[8] G. Ettiene, R. Bauza, R. Plata, M. María, A. Contento, A. Ríos, Electrophoresis 33 (2012) 2969–2977.
[9] K. Starner, K. Goh, Bull. Environ. Contam. Toxicol. 88 (2012) 316–321.
[10] T. Tisler, A. Jemec, B. Mozetic, P. Trebse, Chemosphere 76 (2009) 907–914.
[11] F. Sánchez-Bayo, R. Hyne, Chemosphere 99 (2014) 143–151.
[12] J. Vichapong, R. Burakham, S. Srijaranai, Talanta 117 (2013) 221–228.
[13] W. Wang, Y. Li, Q. Wu, C. Wang, X. Zang, Z. Wang, Anal. Methods 4 (2012) 766–772.
[14] P. Samnani, K. Vishwakarma, S.Y. Pandey, Bull. Environ. Contam. Toxicol. 86 (2011) 554–558.
[15] G.G. Yin, R.S. Kookana, J. Environ. Sci. Health Part B: Pestic. Food Contam. Agric. Wastes 39 (2004) 737–746.
[16] A.M. Rodrigues, V. Ferreira, V.V. Cardoso, E. Ferreira, M.J. Benoliel, J. Chromatogr. A 1150 (2007) 267–278.
[17] S. Seccia, P. Fidente, D.A. Barbini, P. Morrica, Anal. Chim. Acta 553 (2005) 21–26.
[18] D.Q. Thuyet, K. Yamazaki, T.K. Phong, H. Watanabe, D.T.T Nhung, K. Takagi, J. Anal. Chem. 65 (2010) 843–847.
[19] Q. Subhani, Z. Huang, Z. Zhu, Y. Zhu, Talanta 116 (2013) 127–132.
[20] J. L Vílchez, R. El-Khattabi, R. Blanc, A. Navalón, Anal. Chim. Acta 371 (1998) 247–253.
[21] J.L. Vílchez, M.C. Valencia, A. Navalón, B. Molinero-Morales, L.F. Capitán-Vallvey, Anal. Chim. Acta 439 (2001) 299–305.
[22] J. López Flores, A. Molina Díaz, M.L. Fernández de Córdova, Talanta 72 (2007) 991–997.
[23] K. Araujo, G. Ettiene, M. Hernández, A. Cáceres, H. Pérez, Rev. Fac. Agron. (LUZ) 29 (2012) 542–559.
[24] E. Sanchez, B.R. Kowalski, Anal. Chem. 58 (1986) 496–499.
[25] A.C. Olivieri, N.M. Faber, J. Ferré, R. Boqué, J.H. Kalivas, H. Mark, Pure Appl. Chem. 78 (2006) 633–661.
[26] A.C. Olivieri, Chem. Rev. 114 (2014) 5358–5378.
[27] R.G. Zepp, W.M. Sheldon, M.A. Moran, Chemistry 89 (2004) 15–36.
[28] The MathWorks Inc. , MATLAB 6.0, Natick, MA, USA, 2000.
[29] http://www.models.kvl.dk/algorithms.
[30] A.C. Olivieri, H.L Wu, R.Q. Yu, Chemom. Intell. Lab. Syst. 96 (2009) 246–251.
[31] Chemometry Consultancy, /http://www.chemometry.com.
[32] R. Bro, Chemom. Intell. Lab. Syst. 38 (1997) 49–171.
[33] R. Bro, H.L.A. Kiers, J. Chemom. 17 (2003) 274.
[34] D.M. Haaland, E.V. Thomas, Anal. Chem. 60 (1988) 1193–1202.
[35] S.A. Bortolato, J.A. Arancibia, G.M. Escandar, Anal. Chem. 80 (2008) 8276–8286.
[36] M.L. Nahorniak, G.A. Cooper, Y.C. Kim, K.S. Booksh, Analyst 130 (2005) 85–93.
[37] N. Hudson, A. Baker, D. Reynolds, River Res. Appl. 23 (2007) 631–649.